J Mater Sci (2008) 43:2555–2561
DOI 10.1007/s10853-008-2468-6

Thermal properties of ethylene octene copolymer (Engage)/ dimethyldioctadecyl quaternary ammonium chloride-modified montmorillonite clay nanocomposites

Ganesh Latta · Quentin Lineberry · Riko Ozao · Hou-Yin Zhao · Wei-Ping Pan

Received: 16 October 2007 / Accepted: 10 January 2008 / Published online: 20 February 2008

Abstract The nanocomposites of ethylene octene copolymer (Engage®) with an organically modified (dimethyldioctadecyl quaternary ammonium chloride) montmorillonite (M-MMT) clay were synthesized by using a solution intercalation technique. The intercalation of M-MMT layers for M-MMT loading of 2.5–7.5% was verified by the shift of X-ray diffraction peak to a lower angle, showing change in basal d-spacing from 1.26 for M-MMT to 1.35 nm. Internal structure and the dispersion state of M-MMT in the nanocomposites were observed by transmission electron microscope, which confirmed the clay in the intercalated state. Thermomechanical analysis results showed improved dimensional stability under compression at 30 °C for nanocomposites with increasing M-MMT. By DMA, the storage moduli of nanocomposites below glass transition temperature were higher than the neat Engage and increased with increasing M-MMT content. The glass transition temperature was lowest for the nanocomposite containing 2.5% M-MMT (E-2.5M-MMT), suggesting the optimal concentration of M-MMT in nanocomposite being 2.5% or higher from the viewpoint of thermal properties. The oxidation induction time (OIT) of the nanocomposites was obtained by using pressure-differential scanning calorimeter. The Engage/M-MMT nanocomposites were superior in thermal oxidation resistance as compared to the neat Engage, with E-5.0M-MMT yielding highest OIT_{time} value.

G. Latta · Q. Lineberry · R. Ozao · H.-Y. Zhao · W.-P. Pan
Thermal Analysis Laboratory, Institute for Combustion Science and Environmental Technology, Western Kentucky University, Bowling Green, KY 42101, USA

R. Ozao (✉)
SONY Institute of Higher Education, Atsugi, Kanagawa, Japan
e-mail: ozao@aoni.waseda.jp

Introduction

In the past two decades, the research in polymer/layered silicate nanocomposite has attracted the interests of academics and industries due to their improved mechanical, thermal, flame retardation, ablation resistance, and enhanced barrier properties [1–6]. Montmorillonite, more specifically a 2:1 phyllosilicate consisting of layers built by two silica tetrahedral sheets and one octahedral sheet of aluminum or magnesium hydroxide, has been well recognized to improve the mechanical strength and thermal properties of the polymer to which it is added [7–9]. By isomorphic substitution of Al^{3+} by divalent (Fe^{2+} or Mg^{2+}) cations, negative charge is generated, which is counterbalanced with cations such as Li^{+}, Na^{+}, Ca^{2+}. Such layers organize themselves as parallel layers with a regular van der Waals gap (called interlayer or gallery). It is also common to render the originally hydrophilic surface organophilic by exchanging the alkali counterions with cationic organic surfactants such as alkylammoniums [10]. The addition of organically modified montmorillonites (M-MMTs) to polymers further imparts flame retardancy, barrier properties, and ablation resistance to the resulting composite due to nanoscopic distribution and to a synergetic effect of the nano-sized crystals with the polymer chains [11].

Polymer/layered silicate nanocomposites are synthesized by four techniques: in situ polymerization, intercalation from polymer solution, intercalation by polymer melt or melt intercalation, and sol–gel technique [12]. The melt intercalation technique is a low-cost method by which the polymer chain can be intercalated into the galleries of clay by heating the polymer and organo–clay mixture to the glass transition temperature or the melting temperature of polymer. The mobile polymer chain can diffuse into the clay galleries and expand the silicate layer

structure [11]. However, heating to high temperatures may affect the M-MMT and/or the polymer matrix. Bhowmick and coworkers have studied the solution method for the clay-based nanocomposite synthesis of thermoplastic elastomers and rubbers [13–15].

The importance of thermal stability of polymer/montmorillonite nanocomposites has been recently pointed out [4, 16]. The interaction between the MMTs and the polymer matrix is so complicated that the alkyl chain length, number of alkyls, degree of saturation of the organic modifiers affect the thermal properties of the nanocomposites [17]. Hence, the determination of the onset temperature of degradation, as well as the understanding of degradation mechanism and the thermal stability of the nanocomposite are crucial for the practical use of nanocomposites [4].

Engage®, a relatively new copolymer of ethylene and 1-octene, is a commercially available polyolefinic elastomer, which possesses flexibility and mechanical properties of a synthetic rubber and a processability of plastics. For example, Engage has been used to modify the impact strength of polypropylene copolymer [18, 19]. Engage nanocomposites have been prepared using an organic amine-modified clay, and their characterization has been made mainly on mechanical properties [20]. However, to the authors' knowledge, no detailed study has been made on the thermal degradation or the thermal stability of Engage nanocomposites.

Thermal oxidative stability is also useful for assessing shelf life of polymers, and thermal methods, such as differential scanning calorimetry (DSC), have been widely used for obtaining oxidative induction time (OIT_{time}) [21] for this purpose.

Accordingly, the present paper reports the thermal properties of the nanocomposites of ethylene octene copolymer (Engage) with an organically M-MMT. Nanocomposites containing 1, 2.5, 5, and 7.5% dimethyldioctadecyl ammonium chloride were prepared by the solution intercalation method and were first characterized by X-ray diffraction (XRD), Fourier transform infrared spectroscopy (FTIR), and transmission electron microscopy (TEM). Thermal properties were obtained by thermogravimetric analysis (TGA), Pressure-DSC (P-DSC), thermomechanical analysis (TMA), and dynamic mechanical thermal analysis (DMTA). In particular, thermal oxidative stability was evaluated by OIT_{time}.

Material preparation

Materials

Engage®, an ethylene octene copolymer (Manufactured by Dow Chemicals, USA), was obtained from Infiltrator System Inc, KY, USA. An M-MMT clay, SCPX-2052, was supplied by Southern Clay, Inc., USA. Dichlorobenzene was obtained from Fisher Scientific, USA.

Table 1 Designation used for clay and nanocomposites

Name	Designation
Dimethyldioctadecyl quaternary ammonium chloride modified montmorillonite clay	M-MMT
Engage-0% M-MMT	E-0M-MMT
Engage-1%M-MMT	E-1M-MMT
Engage-2.5%M-MMT	E-2.5M-MMT
Engage-5.0%M-MMT	E-5.0M-MMT
Engage-7.5%M-MMT	E-7.5M-MMT

Preparation of polymer–clay nanocomposite

A 10-g portion of the ethylene octene copolymer (Engage) was first dissolved in dichlorobenzene by stirring for 2 h at a temperature range of 80–90 °C. The dimethyldioctadecyl quaternary ammonium chloride modified clay was dispersed in ethanol. The required amount of dispersed clay was poured into polymer solution with constant stirring. The polymer–clay mixture was stirred for 2 h. The solution was taken in PTFE Petri dish and dried in vacuum oven at 80 °C for 48 h. The sheet obtained after drying off the solvent was used for the analysis. Four clay-loaded polymer samples were prepared, each differed in clay loading, i.e., 1, 2.5, 5, and 7.5%. One sheet was prepared in the same manner without any clay, and this sheet was used as a control to compare the properties with the nanocomposites. Table 1 shows the designation of modified clay and nanocomposites.

Experimental

XRD technique

The clay and the nanocomposites were characterized using Thermo-X'TRA XRD diffractometer with Cu Kα radiation ($\lambda = 0.15418$ nm) with the scanning rate of 0.3°/min, operated at a current of 40 mA and a voltage of 45 kV.

Transmission electron microscopy

The microstructure of nanocomposites was imaged using a JEM-100LX, JEOL TEM (JEOL USA, Inc., Peabody, MA, USA) under an accelerating voltage of 200 kV. The Engage/MMT nanocomposite samples were sectioned into ultra thin slices at the temperature of −135 °C using a cryo ultramicrotome equipped with diamond knife and was mounted on copper grid for analysis.

Fourier transform infrared spectroscopy

Fourier transform infrared spectroscopy spectra are obtained from Perkin-Elmer Spectrum One FTIR, in U-ATR mode. The IR detection range was 550–4,000 cm^{-1}, and the resolution of spectrum was 4 cm^{-1}.

Thermogravimetric analysis

Non-oxidative decomposition of the samples was observed by TGA using TA Q-5000 TGA (TA Instruments, New Castle, DE, USA) under 40 mL/min flow of ultra high purity (UHP) grade nitrogen. About 10–15 mg each of the samples was loaded in a platinum sample pan and heated from room temperature to 800 °C at a heating rate of 10 °C/min.

Thermomechanical analysis

Thermal expansion and contraction of Engage/M-MMT nanocomposites were examined by using a TA 2940 TMA (TA Instruments, New Castle, DE, USA) under compression mode with a force rate of 0.1 N/min to 1 N at constant temperature of 30 °C.

Dynamic mechanical thermal analysis

The dynamic mechanical properties including the loss modulus and storage modulus of Engage/M-MMT nanocomposites were obtained by using TA2980 DMA (TA instruments, New Castle, DE, USA). The samples were analyzed in a film tension mode at a constant frequency of 1 Hz, with a strain of 0.01%, in the temperature range of from −70 to 100 °C with the heating rate of 5 °C/min.

Pressure-DSC

Pressure-DSC was used for the determination of OIT of Engage/M-MMT nanocomposite according to ASTM D 3895 [21]. OIT test was performed by using TA Q-20 P-DSC (TA Instruments, New Castle, DE, USA). The sample was equilibrated at 50 °C and then heated to 180 °C with the room temparature rate of 20 °C/min under nitrogen (UHP grade). The sample was kept isothermal for 5 min under nitrogen and then the gas is switch to ultra high pure oxygen at 20 psi pressure and flown at a rate of 50 mL/min, where the sample was kept isothermal for further 20 min for the determination of OIT of each sample.

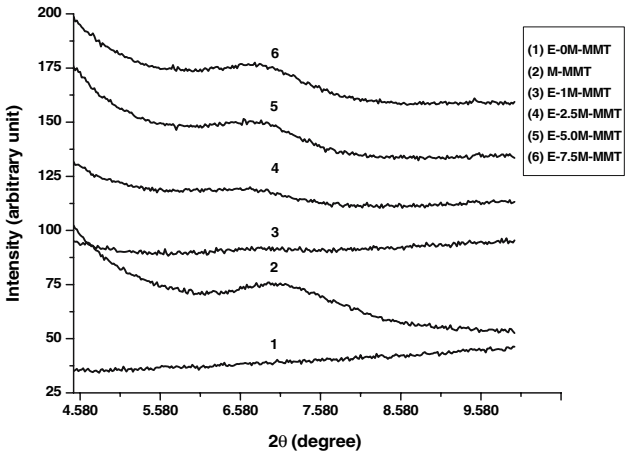

Fig. 1 XRD pattern of M-MMT and Engage/M-MMT containing various clay contents

Results and discussion

X-ray diffraction

The X-ray diffractograms of the modified clay and Engage/modified MMT clay-based nanocomposites are shown in Fig. 1. The 2θ and intergallery spacing of M-MMT and nanocomposites are given in Table 2.

The 2θ value for M-MMT is 6.98° and the corresponding d-spacing is 1.26 nm. The 2θ value for E-2.5M-MMT is 5.56° and the gallery gap is 1.35 nm. The increase in the basal spacing confirms the intercalation of polymer chain in the gallery of M-MMT. Similarly, it can be seen for E-5.0M-MMT and E-7.5M-MMT that the 2θ values are 6.58° and 6.68°, and that the corresponding d-spacings are 1.34 and 1.32 nm, respectively. The highest degree of intercalation was obtained for E-2.5M-MMT nanocomposites; hence, the d-spacing decreases with the increasing amount of clay (E-5.0M-MMT and E-7.5M-MMT).

Transmission electron microscopy

The TEM micrographs of E-2.5M-MMT are shown in Fig. 2a, b. The dispersion of M-MMT within the polymer

Table 2 2θ and gallery spacing of modified clay and nanocomposites

Sample	2θ (degree)	Gallery gap (nm)
M-MMT	6.98	1.26
E-0M-MMT	No peak	–
E-1M-MMT	No peak	–
E-2.5M-MMT	6.56	1.35
E-5.0M-MMT	6.58	1.34
E-7.5M-MMT	6.68	1.32

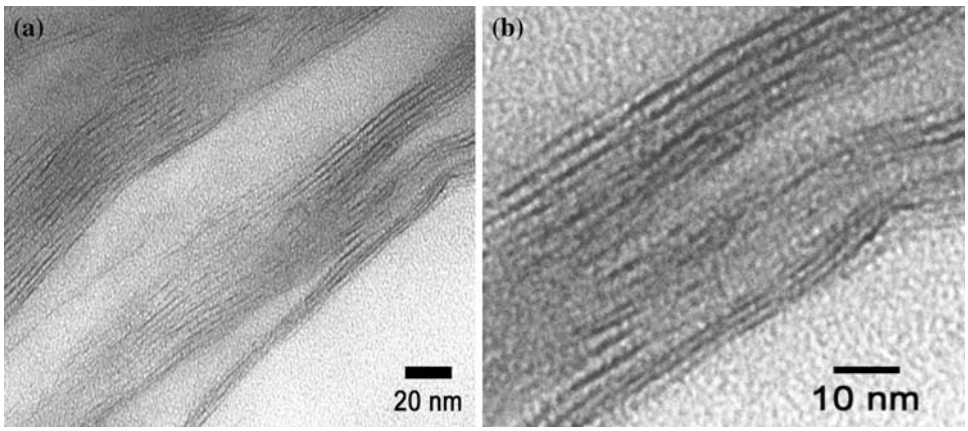

Fig. 2 (**a**, **b**) TEM micrograph of Engage-M-MMT nanocomposite containing 2.5% clay

matrix is shown by TEM micrograph. The dark lines represent each clay layers and the white background corresponds to the polymer matrix. Referring to Fig. 2b, the stacked layer structures of the original M-MMT are found to be separated and finely dispersed. The interlayer spacing of M-MMT in nanocomposite as read from the micrograph is 1.30–1.45 nm, which, as an average, is larger than the original interlayer spacing of the original clay. The observations support the results obtained from XRD (1.35 nm). The average particle width is 30–40 nm for E-2.5M-MMT. The XRD results show the intercalation of clay galleries and the TEM micrograph shows the excellent dispersion of clay to support XRD data.

Fourier transform infrared spectroscopy

Figure 3 shows the FTIR spectra for all the samples. Neat M-MMT clay shows a broad peak in the range of 3,500–3,700 cm^{-1} corresponding to the O–H stretching, and a peak at 1,643 cm^{-1} characteristic for O–H bending. The very strong peak present at 1,002 cm^{-1} in M-MMT corresponds to Si–O–Si stretching. The peaks at around 2,921 and 2,850 cm^{-1} are assigned to the C–H stretching of CH_2 or CH_3 group present in the Engage polymer and in the dimethyldioctadecyl quaternary ammonium chloride, a modifier for the clay. Similarly, C–H bending peak at around 1,467 cm^{-1} can be seen for both Engage and M-MMT. The peaks at 1,375 and 1,300 cm^{-1} for Engage are due to C–H rocking and C–H wagging, respectively. The FTIR spectra of Engage/M-MMT nanocomposites show additional peaks as compared to the neat Engage, i.e., at 1,002 and 1,643 cm^{-1}, which are attributed to M-MMT, and the heights of the peaks increase with increasing loading of M-MMT. These results show that M-MMT is successfully incorporated in the polymer matrix (Table 3).

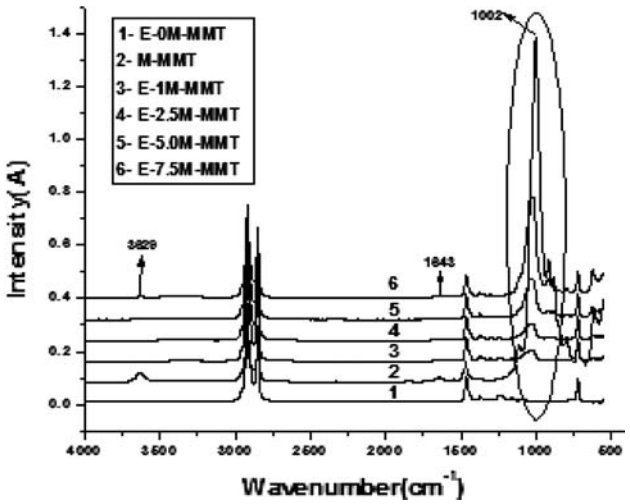

Fig. 3 FTIR spectra of M-MMT, Engage, and Engage-M-MMT nanocomposite

TGA analysis

Figure 4 shows the mass loss pattern of Engage and Engage/M-MMT nanocomposites with heating to 800 °C at a heating rate of 10 °C/min. The onset decomposition

Table 3 FTIR peaks of M-MMT and Engage

Wavenumber (Clay)	Wavenumber (polymer)
3,629	2,914
2,921	2,849
2,850	1,465
1,643	1,375
1,467	1,300
1,114	1,244
1,002	1,157
916	719
883	797
722	
619	

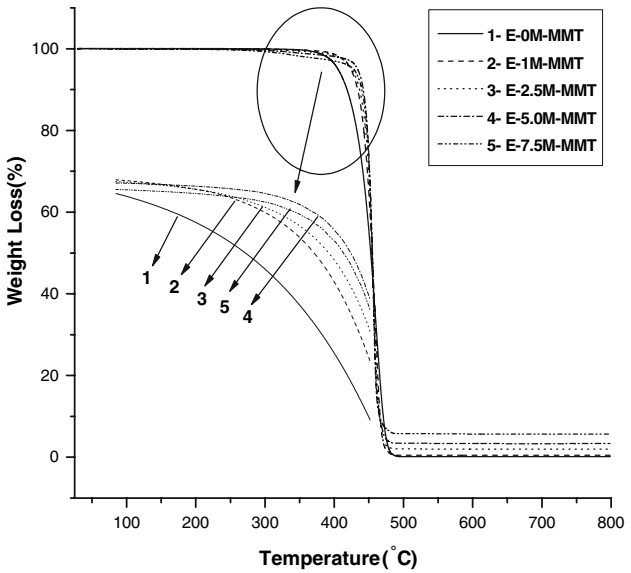

Fig. 4 TGA thermogram of Engage and Engage/M-MMT nanocomposites

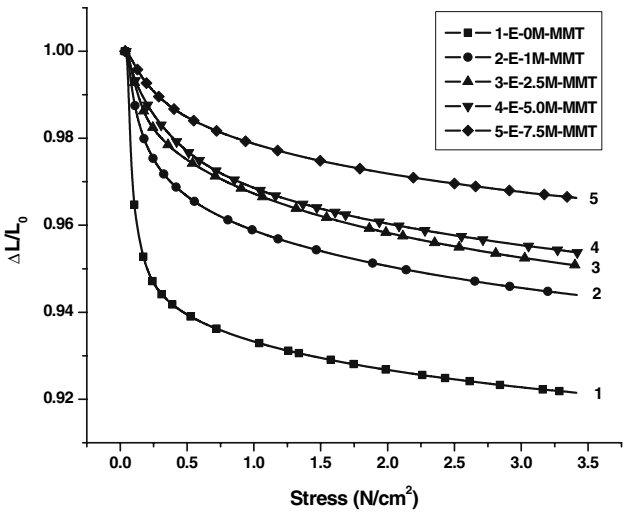

Fig. 5 Dimensional stability at 30 °C of Engage and Engage/M-MMT nanocomposite shown by normalized compression ratio and normalized pressure

and temperature at 5% weight loss of Engage and nanocomposites are given in Table 4. It is evident that the degradation temperature of neat Engage is lower than the Engage/M-MMT nanocomposite. The degradation temperature of nanocomposite increases with increasing clay loading up to 5% and then decreases for 7.5% clay-loaded composite. The homogeneous dispersion clay in polymer matrix and the intercalation of polymer chain in the clay galleries presumably account for the improvement in thermal degradation resistance of the nanocomposites. The decrease in thermal degradation for E-7.5M-MMT might be due to the agglomeration of clay in polymer matrix. Ding et al. [22], studied PP nanocomposites with organically modified MMTs and reported that the initial thermal stability of the matrix increased with increasing MMT content to 4 phr, but then decreased with further increasing the addition of MMTs, at which partial exfoliation of the clay layers was observed.

Table 4 Onset decomposition temperature of Engage/M-MMT nanocomposites

Sample	Temperature at 5% weight loss (°C)	Onset decomposition (°C)
E-0M-MMT	405	415
E-1M-MMT	425	433
E-2.5M-MMT	426	440
E-5.0M-MMT	434	448
E-7.5M-MMT	429	443

TMA analysis

Thermomechanical analysis runs were carried out under compression mode at a constant temperature of 30 °C, and the results are summarized in Fig. 5, where normalized dimensional change (dimensionless) and compaction pressure P (MPa) are defined by Eqs. 1 and 2, respectively:

$$E = \Delta L/L_0, \tag{1}$$

where, L_0 (μm) is the compaction length of the neat polymer, and ΔL, (μm) is the difference in length from the initial length for each composite, and

$$P = F/S \tag{2}$$

where, F (N) is the force applied vertically to the sample, and S (cm^2) is the cross-sectional area of the applied force.

The onset point for the compaction pressure for the samples is given in Table 5. With increasing M-MMT loading in nanocomposites, the onset point increases, whereas the dimensional change decreases. This shows the improved dimensional stability for nanocomposites with increasing M-MMT content, which is attributed to the reinforcing effect of the nanoparticles of M-MMT.

Table 5 Dimensional change and force onset point for Engage and Engage/M-MMT nanocomposites

Sample	Dimensional change up to onset point (μm)	Onset point for pressure (N/cm^2)
E-0M-MMT	58.70	0.11
E-1M-MMT	33.66	0.18
E-2.5M-MMT	32.04	0.21
E-5.0M-MMT	28.76	0.28
E-7.5M-MMT	23.46	0.35

Table 6 T_g for the samples as read from tan δ peaks

Sample	Glass transition temperature (°C)
E-0M-MMT	−29.7
E-1M-MMT	−30.3
E-2.5M-MMT	−31.3
E-5.0M-MMT	−31.1
E-7.5M-MMT	−30.9

DMTA analysis

In Table 6 are tabulated the glass transition temperature, *T*g, obtained from tan δ versus temperature. Figures 6 and 7 show plots of storage modulus and tan δ plots with respect to temperatures. The glass transition temperature, *T*g, is lowest for E-2.5M-MMT and E-5.0M-MMT. The shift of *T*g to the lower temperature side indicates that the molecules are of relatively low molecular weight because the mobility of the molecules is affected by the terminal groups. Below the glass transition temperature, the storage modulus of neat polymer is lower than the nanocomposites (Fig. 6), and it increases with increasing loading of M-MMT up to 7.5% M-MMT. At *T*g, the polymer chain gains the mobility and dissipates the energy in viscous medium. The relative height of tan δ peak for the composites with respect to the peak height for E-0M-MMT decreases with increasing amount of M-MMT from 1 to 0.76 for E-7.5M-MMT, and it is related to the volume of constrained chains [23]. For instance, the volume of the constrained chains for E-2.5M-MMT and E-7.5M-MMT is 11 and 24%, respectively, and this shows that the number of mobile chains decreases with increasing clay loading. The tan δ peak for E-5.0M-MMT is almost the same as that for E-2.5M-MMT, but for E-7.5M-MMT, the height and area of tan δ peak decreases whereas the peak temperature increases (Fig. 7). These suggest an increased polymer–M-MMT interaction, thus reducing the number of available free chains in the matrix polymer [24]. This tendency is the same as evaluated by TMA. That is, the dimensional stability is highest for E-7.5M-MMT. Furthermore, an additional small peak is observed in the tan δ curve of E-2.5M-MMT and E-7.5M-MMT, which may suggest phase separation.

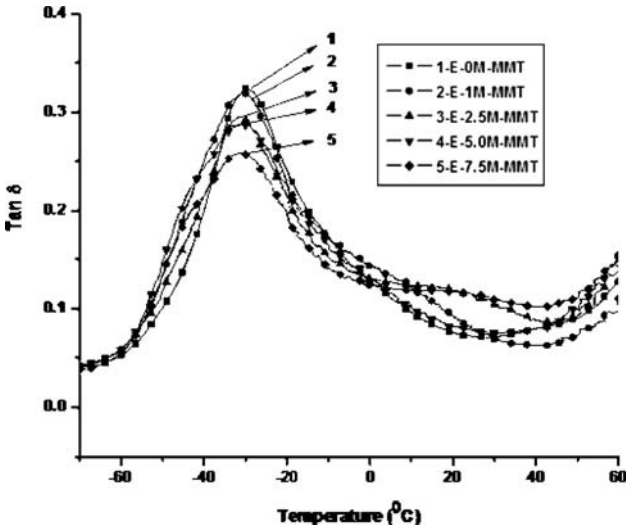

Fig. 7 Tan δ of Engage/M-MMT nanocomposites containing various clay loading

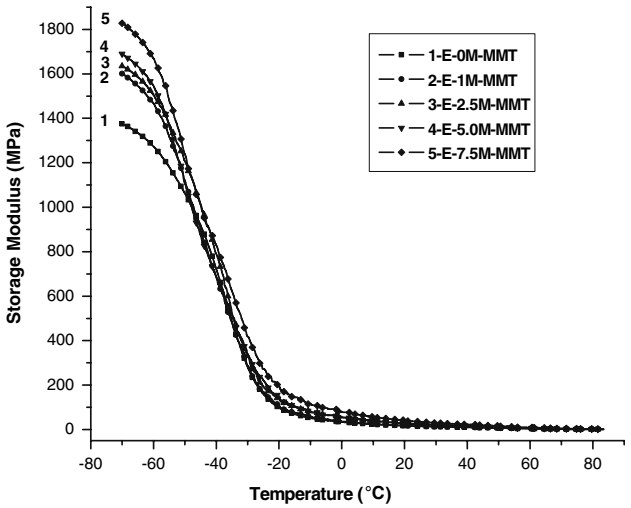

Fig. 6 Storage modulus of Engage/M-MMT nanocomposites containing various clay loading

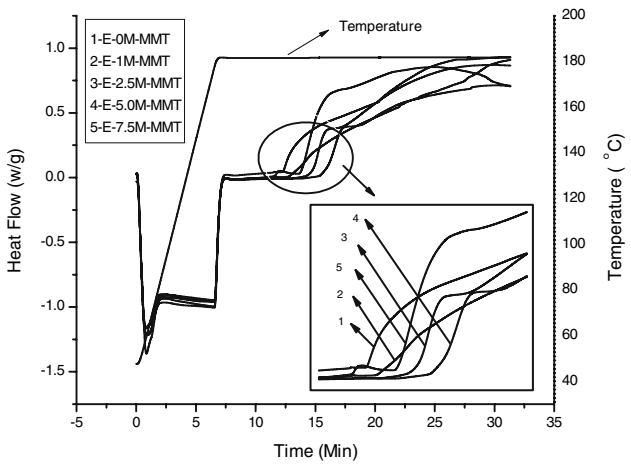

Fig. 8 P-DSC curves for obtaining Oxidation induction time of Engage and Engage/M-MMT nanocomposite containing various M-MMT contents

Table 7 Oxidation induction time of Engage and Engage/M-MMT nanocomposite containing various M-MMT contents

Sample	Oxidation induction time (min)
E-0M-MMT	12.31
E-1M-MMT	12.87
E-2.5M-MMT	14.77
E-5.0M-MMT	15.85
E-7.5M-MMT	13.82

Pressure-DSC analysis

Figure 8 shows the DSC thermograms of the samples for obtaining the OIT_{time}. The OIT_{time} of each sample is listed in Table 7. It is evident that the OIT_{time} of Engage increases with the increasing amount of M-MMT incorporated in the polymer. The decrease in OIT_{time} for E-7.5M-MMT is probably due to the poor dispersion and agglomeration of M-MMT in polymer matrix. The exotherm before the oxidation of E-7.5M-MMT nanocomposite may be ascribed to the oxidation of modifier of agglomerated clay; however, studies on degradation mechanism are required for clear understanding. The OIT_{time} value of E-5.0M-MMT was highest between the neat Engage and other clay-loaded nanocomposites. For E-5.0M-MMT, the improvement in OIT_{time} is presumed due to the intercalation of clay layers by polymer chain and uniform dispersion of M-MMTs as described above. As evaluated hereinbefore by TGA, E-5.0M-MMT showed higher thermal stability under non-oxidizing conditions and even under such dynamic heating conditions, it is likely that the initiation of the reaction is also retarded particularly in the case the mobility of the polymer chains are limited as shown by the lower glass transition temperature for E-5.0M-MMT.

Conclusion

Nanocomposites of an ethylene octene copolymer (Engage®) with an M-MMT clay were prepared by solution technique. Intercalation of M-MMT with polymer chains to an interlayer distance of 1.35 nm was successfully observed by XRD analysis and TEM observations for samples containing 2.5% or more M-MMT. TMA results showed the improved dimensional stability for nanocomposite at 30 °C with increasing M-MMT content to 5.0%. The dimensional stability under compression increases with the increasing clay loading of nanocomposites. The storage moduli of nanocomposites below glass transition temperature were higher than the neat Engage and increased with increasing M-MMT content. The glass transition temperature was lowest for the nanocomposite containing 2.5% M-MMT (E-2.5M-MMT), suggesting the optimal concentration of M-MMT in nanocomposite being 2.5% or higher from the viewpoint of thermal properties. The Engage/M-MMT nanocomposites were superior in thermal oxidation resistance as compared to the neat Engage, and among them, E-5.0M-MMT showed highest OIT_{time} value.

Acknowledgements We would like to acknowledge Dr Karren Leslie More and Shawn Reeves of Oak Ridge National Laboratory for helping us in the cryo-microtoming of samples by share facility. We would also like to acknowledge Jon Andersland of Biology Department, Western Kentucky University, for helping in TEM results of nanocomposite. We are grateful to Peter Inch of Infiltrator Systems Inc., for providing Engage polymer sample for our research work. The authors also acknowledge LECO Professorship, Applied Research and Technology Program at Ogden College, NASA Graduate Student Research Program (GSPR-NGT1-03012), and Sumpter Professorship to provide financial support for this project.

References

1. Utracki LA (2004) Clay-containing polymeric nanocomposites. RAPRA Tech Ltd., Shawbury, UK
2. Oya A, Kurokawa Y (2000) J Mater Sci 35:1045
3. Njuguna J, Pielichowski K (2003) Adv Eng Mater 5:769
4. Leszczynska A, Njuguna J, Pielichowski K, Banerjee JR (2007) Thermochim Acta 453:75
5. Njuguna J, Pielichowski K (2004) Adv Eng Mater 6:193
6. Njuguna J, Pielichowski K (2004) Adv Eng Mater 6:204
7. Kato M, Usuki A, Okada A (1997) J Appl Polym Sci 66:1781
8. Kawasumi M, Hasegawa N, Kato M, Usuki A, Okada A (1997) Macromolecules 30:6333
9. Hasegawa N, Kawasumi M, Kato M, Usuki A, Okada A (1998) J Appl Polym Sci 67:87
10. Giannelis EP, Krishnamoorti R, Manias E (1998) Adv Polym Sci 138:107
11. Vaia RA, Giannelis EP (1997) Macromolecules 30:8000
12. Sinha Ray S, Okamoto M (2003) Prog Polym Sci 28:1539
13. Sadhu S (2004) J Appl Polym Sci 92:698
14. Acharya H, Srivastava SK, Bhowmick AK (2006) Poly Sci Eng 46:837
15. Ganguly A, De Sarkar M, Bhowmick AK (2006) J Appl Polym Sci 100:2040
16. Leszczynska A, Njuguna J, Pielichowski K, Banerjee JR (2007) Thermochim Acta 454:1
17. Xie W, Gao Z, Liu K, Pan W-P, Vaia R, Hunter D, Singh A (2001) Thermochim Acta 367–368:339
18. Paul S, Kale DD (2000) J Appl Polym Sci 76:1480
19. Lim JW, Hassan A, Rahmat AR, Wahit MU (2006) J Appl Polym Sci 99:3441
20. Maiti M, Sadhu S, Bhowmick AK (2006) J Appl Polym Sci 101:603
21. ASTM D-3895 (1995) Standard methods for oxidation-induction time of polyolefins by differential scanning calorimetry
22. Ding C, Hui He DJ, Guo B, Hong H (2005) Polym Test 24:94
23. Rao YQ, Pochan JM (2007) Macromolecules 40:290
24. Jha A, Bhowmick AK (1997) Rubber Chem Technol 70:798